A Well-Being-Centric Walkable Tourism Platform Using AI Agent

Anna Yokokubo[1*], Yusuke Sasaki[2*], Takeo Hamada[1], Yoshio Ishiguro[1], Lidia Vitanova[3],
Denis Dimitrov[3], Dessislava Petrova-Antonova[3], Sylvia Ilieva[3], Noboru Koshizuka[1]

[1]Interfaculty Initiative in Information Studies, The University of Tokyo, 113-0033 Bunkyo Tokyo, Japan -
{anna.yokokubo, htakeo, yoshio.ishiguro, noboru.koshizuka}@iii.u-tokyo.ac.jp
[2]Graduate School of Interdisciplinary Information Studies, The University of Tokyo, 113-0033 Bunkyo Tokyo, Japan -
yusuke.sasaki@koshizuka-lab.org
[3]GATE Institute, Sofia University, Bulgaria –
{lidia.vitanova, denis.dimitrov, dessislava.petrova, sylvia}@gate-ai.eu

Keywords: Well-being, AI Agent, Heat-Aware Routing, Walkability, Personalised Route Recommendation, Urban Data Integration

Abstract

We propose a Well-Being-Centric Walkable Tourism Platform Using AI Agent that fuses heterogeneous urban data—an OSM pedestrian graph, a city-scale microclimate field, and a walkability layer for Sofia, Bulgaria—with an AI agent that converts free-text user requests into a constrained heat-aware routing problem. The platform addresses a gap in existing digital map services, which offer rich navigation but lack integrated support for well-being-oriented urban exploration under intensifying urban heat islands. The routing engine implements two complementary strategies: P2, a ρ-detour-constrained heat-aware route obtained by Lagrangian relaxation, and PLLM, in which a large language model maps the user's chat message and current temperature to a bounded detour budget ρ fed into the same engine. In a systematic evaluation over a POI grid in central Sofia, heat-aware routes consistently reduced cumulative heat exposure with only marginal detours, outperforming both the shortest-distance baseline and the heat-blind Google Directions API, while PLLM adaptively selected detour budgets matching user personas. We further conducted a subjective field study with local residents in Bulgaria, comparing the baseline shortest route with the proposed heat-aware route. The results indicated that the proposed routes were consistently feasible for walking and were perceived as more comfortable and scenically pleasant in several segments.

1. Introduction

Tourists increasingly rely on guidebooks, online platforms, and social media to plan their trips. Such information sources tend to concentrate visitors at popular destinations, producing imbalanced crowd distribution and diminished tourism experiences. At the same time, urban heat islands and global warming are turning summer walking in Mediterranean and continental European cities into a public-health concern: prolonged exposure to high apparent temperature degrades both comfort and physical capacity, especially for the elderly and for international visitors who are not acclimatised (Huber et al., 2025, Ma et al., 2025). Existing digital map services provide rich navigational information but offer little integrated support for well-being-oriented urban exploration that simultaneously accounts for walkability, heat avoidance, and individual physical condition.

With advances in smart-tourism technologies, data-driven methods have been increasingly adopted. Real-time visualisation of crowd congestion and predictive analytics based on tourist behaviour have been developed to support dynamic destination management (Gretzel et al., 2020). These systems enable both tourists and city managers to make informed decisions by leveraging large-scale urban and mobility data. To mitigate overtourism, several approaches encourage travel during off-peak seasons and guide visitors toward less-explored areas alongside flagship destinations (Honey and Frenkiel, 2021, Peeters et al., 2018, UNWTO, 2018). A complementary line of work emphasises personalised tourism by incorporating individual preferences and contextual information into on-site guidance (Isoda et al., 2020), and gamification-based approaches have been explored to nudge tourists toward less crowded areas while improving engagement (Kawanaka et al., 2020, Matsuda et al., 2022).

These studies highlight the importance of integrating destination management strategies with user-centric design to achieve both efficient resource utilisation and enhanced tourist experiences. However, existing approaches typically treat these aspects separately, and few systems treat *thermal comfort* as a first-class routing constraint that the user can negotiate in natural language.

To address these gaps, we propose a Well-Being-Centric Walkable Tourism Platform that fuses urban data and an AI agent to deliver personalised, heat-aware tourism experiences. The platform integrates heterogeneous data sources – a high-resolution pedestrian graph, a city-scale microclimate field, a walkability index, and per-segment metadata – and exposes a Tourism AI Agent that performs conversational guidance, itinerary planning, and route recommendation through versioned APIs. Internally, the agent reduces every routing request to a constrained shortest-path problem in which a Lagrangian multiplier λ trades off cumulative heat exposure against detour length, and a large language model (LLM) infers a user-facing detour budget ρ from the chat message and the current temperature.

The contributions of this paper are:

- A reproducible heat-aware routing pipeline (section 3) defined as a ρ-detour-constrained Lagrangian relaxation

[*]These authors contributed equally to this work.

on a NetworkX/OSMnx pedestrian graph, with three interchangeable cumulative heat exposure metrics (T2, Thom Discomfort Index, WBGT) sharing the same code path.

- A LLM-driven preference-to-budget mapping (PLLM, section 3.4) that converts free-text requests such as "it's so hot, please take me through shade" into a single user-facing parameter $\rho \in [1.0, 1.5]$, with a deterministic heuristic fallback for offline use.

- A full-grid quantitative evaluation (section 4) on 1,584 OD cases in central Sofia, comparing the proposed methods against a shortest-distance baseline (B1) and a heat-blind external reference (B-ext, the Google Directions API). All paired tests achieve $p < 10^{-17}$ after Holm-Bonferroni correction.

- A supplementary partner-route analysis (section 4.3) on five waypoint-constrained corridors (840 cases, $\rho \in \{1.0, 1.05, 1.10, 1.15, 1.20\}$) that localises zone-dependent ρ sensitivity on routes residents actually walk.

- A subjective evaluation protocol (section 4.4) with three Sofia-based walkers across three partner-proposed walking pairs and two transit pairs (GW1–GW3, GT1–GT2), including a participant-drawn "how would you go on a hot day?" route to verify that the LLM-chosen ρ aligns with how locals actually navigate summer heat.

2. Related Work

Heat-aware pedestrian routing. Recent work confirms that pedestrians in hot cities actively trade distance for thermal comfort (Melnikov et al., 2022). (Ma et al., 2025) generated more than 2.2 million pedestrian routes in subtropical Hong Kong and showed that a thermal-discomfort-driven route outperforms the shortest path for 81% of OD pairs, reducing PET-based discomfort by up to 96%, with effectiveness saturating around a 110% detour budget – consistent with our ρ range. (Huber et al., 2025) extended isochrone-based accessibility analysis with a heat-sensitivity layer in Heidelberg, demonstrating that under high heat-stress conditions a substantial fraction of the population becomes effectively excluded from essential services. Both works rely on rule-based weights or fixed heat-detour ratios; we extend the formulation to a tunable detour budget that can be selected by an LLM from natural language.

Smart and well-being-aware tourism. Smart-tourism research has investigated personalised itinerary planning based on user interests, visit durations, and dynamic conditions such as queuing time and weather (Gretzel et al., 2020, Isoda et al., 2020, Lim et al., 2015) as well as interactive planning, gamification, and participatory sensing (Yahi et al., 2015, Kawanaka et al., 2020, Matsuda et al., 2022). These approaches do not jointly optimise navigation and well-being constraints in real time. Mobility-impact studies under heat (Melnikov et al., 2022) confirm that thermal comfort modulates route choice, motivating its inclusion as a first-class constraint in tourism platforms.

Constrained shortest-path and LLM-augmented planning. The detour-constrained heat-aware problem is a delay-constrained shortest path (Jüttner et al., 2001). We solve it via Lagrangian relaxation with binary search on λ, layered on top of standard Dijkstra search (Dijkstra, 1959). Retrieval-augmented generation (Lewis et al., 2020) has popularised the use of LLMs as orchestrators of structured downstream tools. More recently, LLMs have also been employed to transform vague natural-language preferences into well-defined optimization problems that are subsequently solved by deterministic optimization engines (Kuroki et al., 2026). Our approach combines these ideas but adopts a more constrained interaction: the LLM emits only a single bounded scalar ρ, which is then verified and consumed by a deterministic routing solver. This design retains safety and reproducibility while enabling intuitive natural-language interaction.

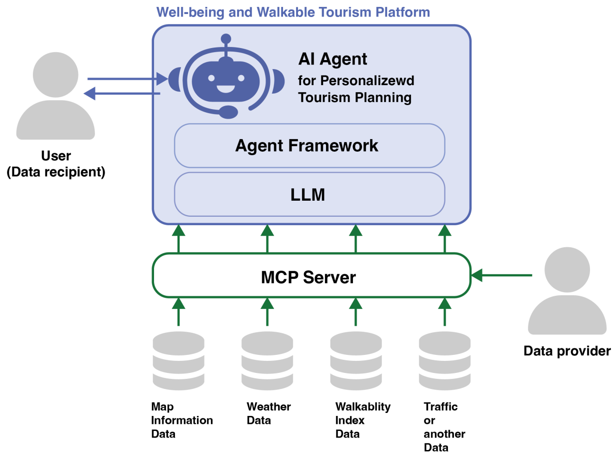

Figure 1. Architecture of the Well-being and Walkable Tourism Platform

3. Development of a Well-Being-Centric Walkable Tourism Platform

3.1 System architecture

We propose a Well-Being-Centric Walkable Tourism Platform that leverages urban data and an AI agent to deliver personalized tourism experiences (Figure 1). The proposed platform is designed to integrate diverse data sources, including map information, weather data, traffic conditions, and a walkability index. Building on such heterogeneous urban data, the platform generates routes optimized for each user's individual context, aiming to enhance both user satisfaction and urban sustainability. A key feature of the platform is its Tourism AI Agent, which provides conversational guidance, itinerary planning, and route recommendations through an API. The platform is further intended to incorporate advanced techniques such as retrieval-augmented generation (RAG) and federated learning, enabling scalable and privacy-aware data utilization.

To validate the proposed platform, we implemented a prototype system organized into a three-layer architecture consisting of a *Data-Provider Layer*, a *Platform Layer*, and a *User Interaction Layer* (Figure 2).

The *Data-Provider Layer* supplies heterogeneous urban data for Sofia City, provided in collaboration with a local partner institute. It includes (a) OpenStreetMap pedestrian network data (OpenStreetMap contributors, 2024), (b) hourly microclimate fields (T2, dewpoint, WBGT (See Figure 3)) on a regular grid, and (c) a coarse per-segment walkability proxy derived from OSM highway class and slope.

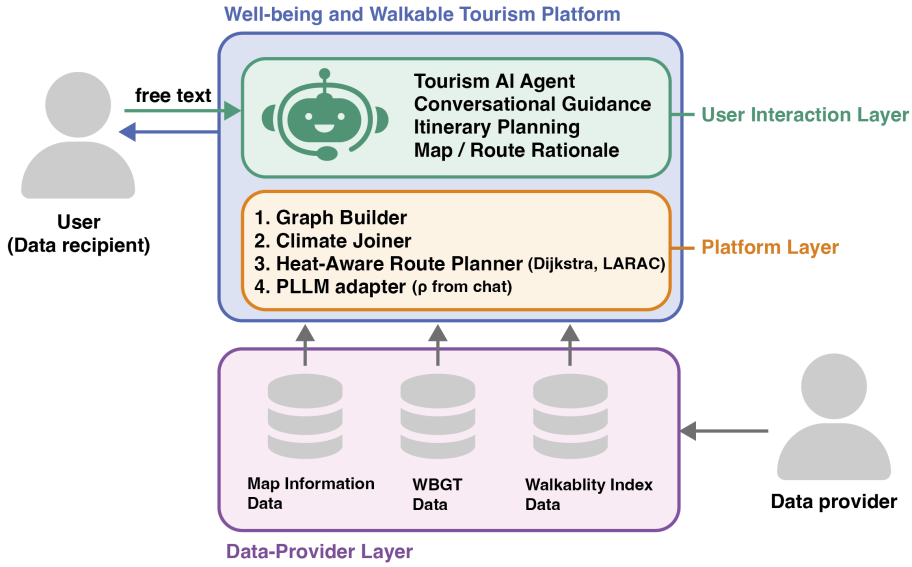

Figure 2. Three-layer architecture of the proposed Well-Being-Centric Walkable Tourism Platform. Heterogeneous urban data feed a stateless platform layer that hosts the heat-aware route planner (Dijkstra + LARAC) and the PLLM adapter (chat $\rightarrow \rho$); a Tourism AI agent then exposes the result to the end user as conversational guidance.

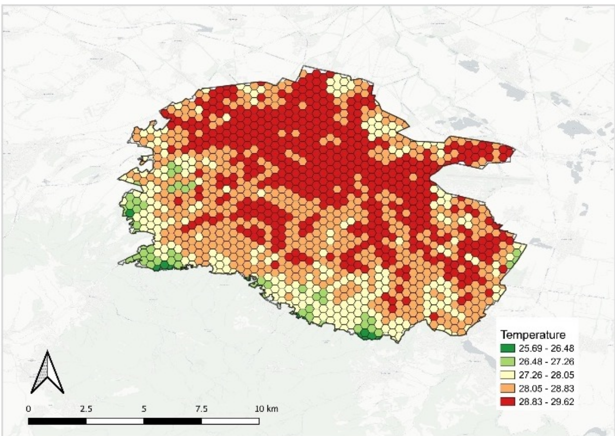

Figure 3. The wet-bulb globe temperature (WBGT) at 15LST on 15th July 2024 in Sofia, Bulgaria.

The *Platform Layer* ingests these inputs, transforms them into an attributed multi-directed pedestrian graph, computes derived indicators such as walkability gain and cumulative heat exposure, and exposes them through a stateless FastAPI service. Each service component (graph builder, climate joiner, route planner, LLM adapter) is a separate module, supporting modular extension to new data sources (e.g., transit, crowd flow).

The *User Interaction Layer* is a Tourism AI Agent: it interprets free-text requests, dispatches them to the route planner with the appropriate detour budget, and returns an interactive map together with a textual rationale.

3.2 Data sources and graph construction

Pedestrian graph. We download the OSM `walk` network for a bounding box around central Sofia (42.640–42.715°N, 23.290–23.380°E) using `OSMnx` (Boeing, 2017) and represent it as a NetworkX (Hagberg et al., 2008) `MultiDiGraph` with 34,639 nodes and 96,216 directed edges. Each edge e carries a length ℓ_e (m) and a baseline walking duration τ_e (s) computed at $1.4\,\mathrm{m\,s^{-1}}$.

Climate field. The microclimate field is encoded as a regular-grid `ClimateGrid` object with hourly slices of T2 (2 m air temperature), dewpoint, and WBGT. Each slice is sampled at the midpoint of every edge to assign a heat-exposure rate $\mathrm{HE}_e(t)$:

$$\mathrm{HE}_e(t) = \begin{cases} \max(0, T2_e(t) - T_{\mathrm{comf}}) & \text{(T2)} \\ \max(0, \mathrm{Thom}_e(t) - T_{\mathrm{comf}}) & \text{(Thom)} \\ \max(0, \mathrm{WBGT}_e(t) - T_{\mathrm{comf}}) & \text{(WBGT)} \end{cases} \tag{1}$$

where the Thom Discomfort Index (Thom, 1959) and WBGT (Yaglou and Minard, 1957) are recomputed from T2 and dewpoint following (Lemke and Kjellstrom, 2012). We use $T_{\mathrm{comf}} \in \{22, 30\}$ °C to study a moderate (t_{comf}=22) and a hot-spot focus (t_{comf}=30) regime.

Walkability layer. A scalar walkability score $w_e \in [0, 1]$ is attached to each edge, derived from the partner walkability product. It is used as a secondary objective in the P2w extension (section 3.3)and is reported as *walkability gain* in the evaluation.

3.3 Heat-aware routing formulation

We formulate route choice as a constrained shortest-path problem. For an OD pair (s, d), time slice t, and edge cost

$$c_e(\lambda, t) = \mathrm{HE}_e(t) \cdot \tau_e + \lambda \cdot \ell_e, \tag{2}$$

we seek the path P minimising $\sum_{e \in P} c_e(\lambda, t)$. The Lagrangian multiplier $\lambda \geq 0$ trades off cumulative heat exposure against length. Two reference operating points bracket the trade-off: $\lambda \to 0$ yields the heat-only route (most detour, largest exposure reduction), while $\lambda \to \infty$ recovers the shortest-distance baseline B1.

In practice users do not specify λ directly; they specify a tolerable *detour ratio* $\rho \in [1.0, 1.5]$, and our P2 method searches for the smallest $\lambda^\star$ such that the resulting path satisfies $\ell(P) \leq \rho \cdot \ell(B1)$. We implement this via the LARAC scheme (Jüttner et al., 2001): after a binary search on λ, we return the heat-aware path that maximally exploits the detour budget. When $\rho = 1.0$, P2 collapses to B1; when ρ is larger than the realised detour of the heat-only path, P2 collapses to the λ=0 solution.

A walkability-aware extension P2w adds a per-edge term $-\beta \cdot w_e$ to Eq. (2); we report it for completeness but use heat-aware-only routes (P2) as the default in this paper.

3.4 LLM-driven preference inference (PLLM)

The PLLM module bridges natural language and the routing engine. Given a chat message m and the current temperature T, it produces a single bounded number $\rho \in [1.0, 1.5]$. Internally, the LLM emits a structured response containing a normalised *heat sensitivity* $s \in [0, 1]$ together with a short rationale; we then map s to ρ via the affine relation

$$\rho(s) = \rho_{\min} + s \cdot (\rho_{\max} - \rho_{\min}), \quad \rho_{\min} = 1.0,\ \rho_{\max} = 1.5. \tag{3}$$

A deterministic heuristic acts as a fallback when LLM access is unavailable: it parses heat-related (“hot”, “shade”, “cool”, their Japanese / Bulgarian counterparts) and hurry-related (“hurry”, “shortest”) cues, weights them, and combines them with a temperature-driven base sensitivity. The hurry weight is intentionally strong (-0.55 per cue) so that explicit hurry intent collapses s to 0 even on hot days, returning $\rho = 1.0$ (i.e., B1). Both backends share the same downstream interface, and the resulting ρ is fed into the same P2 solver. This keeps the LLM *advisory* – it can only choose a parameter inside a safe bounded range and cannot bypass the routing logic, which is important for both reproducibility and safety.

Heuristic vs LLM agreement. Across a 10-persona $\times$ 4-temperature consistency benchmark (multi-lingual phrasings, plus conditional and sarcastic edge cases), the deterministic heuristic alone reaches a 72.5% three-way classification accuracy (*hurry* / *neutral* / *heat-averse*). The remaining errors are concentrated on (a) low-temperature heat-averse phrasings where the temperature term dominates, and (b) Bulgarian / conditional sentences whose cues are not in the keyword list. We expect a calibrated LLM call to recover most of those cases at inference time while the heuristic guarantees the offline / reproducible lower bound.

4. Evaluation

4.1 Experimental setup

Test grid. We use a 12-POI test grid in central Sofia spanning religious, cultural, historical, and park sites (Alexander Nevsky, Vitosha Boulevard, the Largo, Sveta Nedelya, Banya Bashi, Central Baths, NDK, Borisova Gradina, South Park, St. George Rotunda, Ivan Vazov Theatre, City Garden). All $\binom{12}{2} = 66$ OD pairs are evaluated at four hours per day (10, 13, 15, 18 LST) over six days in July 2024, yielding $66 \times 4 \times 6 = 1{,}584$ cases per heat-exposure metric and per T_{comf}.

Methods compared.

- **B1** (shortest distance): Dijkstra on ℓ_e only.
- **B-ext** (Google Directions, walking mode): an external heat-blind reference fetched once and aligned to the same OSM graph.
- **P2** ($\rho \in \{1.05, 1.10, 1.20\}$): ρ-detour-constrained heat-aware route via LARAC.
- **Pρ sweep**: a λ-sweep that traces the entire detour-vs-exposure Pareto frontier; presented as an analytical *solution map*, not a deployable policy.
- **PLLM**: chat persona $\to \rho$ via heuristic / LLM, then P2.

Metrics. For each path P we report: the cumulative heat exposure $\mathrm{HE{\cdot}time}(P) = \sum_e \mathrm{HE}_e \cdot \tau_e$, the average time-weighted heat exposure $\overline{\mathrm{HE}}_t(P) = \mathrm{HE{\cdot}time}(P)/\mathrm{duration}(P)$, the detour ratio $\rho_{\mathrm{realised}}(P) = \ell(P)/\ell(B1)$, the relative reduction $r(P) = (\mathrm{HE{\cdot}time}(B1) - \mathrm{HE{\cdot}time}(P))/\mathrm{HE{\cdot}time}(B1)$, and the walkability gain $\overline{w}(P) - \overline{w}(B1)$. Statistical comparisons against B1 use paired Wilcoxon tests, paired t-tests, Cohen's d for paired samples, and Holm-Bonferroni correction across the K heat-aware methods being compared simultaneously (Holm, 1979).

4.2 Quantitative results

Figure 4 summarises the same-graph, full-grid methods on a single (ρ_{realised}, r) plane: B1 sits at the origin (1.0, 0%), the Pρ sweep traces a smooth Pareto curve that saturates at $\rho \approx 1.045$ (since the heat-only path in central Sofia is itself only $\approx 4.5\%$ longer than B1), and P2 at $\rho_{\max} \in \{1.05, 1.10, 1.20\}$ realises operating points along that curve. B-ext is omitted because its large negative reduction compresses this operating region, and PLLM is shown separately in Figure 6 because its persona experiment uses a smaller OD sample. B-ext remains reported as an external reference in Table 1.

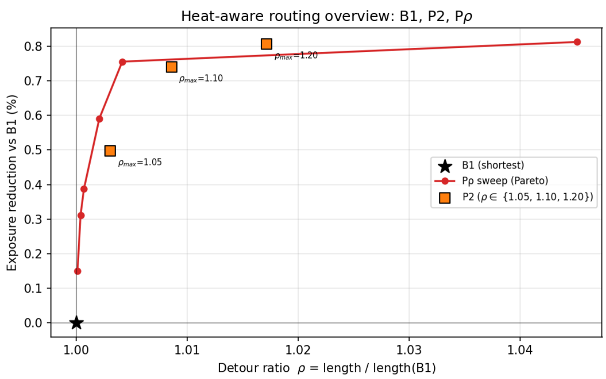

Figure 4. Same-graph, full-grid heat-aware routing overview at T_{comf}=30°C. The Pareto frontier (red) connects B1 (*star*) with the heat-only end, and orange squares are P2 operating points. B-ext and the smaller-sample PLLM experiment are reported separately.

Table 1 reports the headline numbers. P2 shows a smooth, statistically significant exposure reduction with detour budget, peaking near $\rho_{\max} = 1.20$ at a 0.81% reduction with a realised detour of only 3.2% on average. The improvement saturates because central Sofia has limited spatial heat contrast: the heat-only path is itself only $\approx 4.5\%$ longer than B1, so detours larger than $\sim$5% yield no further benefit. The Pareto frontier (Figure 5) makes this saturation explicit. The heat-blind B-ext

Method	$\rho_{\max}$	$\bar{\rho}_{\mathrm{real.}}$	$\bar{r}$ (%)	d_{Cohen}
B-ext (Google)	–	1.104	-11.2	–
P2	1.05	1.003	+0.50	-0.26
P2	1.10	1.009	+0.74	-0.28
P2	1.20	1.017	+0.81	-0.28
Pρ (heat-only end)	–	1.045	+0.81	-0.28
PLLM (hurry persona)	1.00	1.000	+0.00	–
PLLM (heat-averse persona)	1.47	1.003	+0.37	–

Table 1. Mean realised detour and exposure reduction vs B1 (n=1584 paired OD cases, T_{comf}=30°C). All Holm-corrected paired-Wilcoxon and paired-t p-values for heat-aware methods are below 10^{-17}; B-ext is a heat-blind external reference.

incurs an 11% larger walking distance *and* an 11% higher cumulative heat exposure than B1 – a regression that practitioners would not observe by looking at distance alone, but which the Pρ frontier exposes immediately.

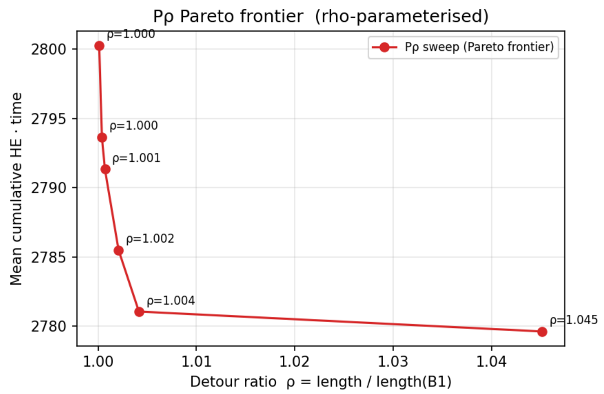

Figure 5. Pρ Pareto frontier obtained by sweeping the Lagrangian multiplier on the same 1,584 OD cases. Each point is labelled with the realised mean detour ratio.

Language-driven ρ selection. The reproducible PLLM persona experiment (Figure 6, six personas × 10 OD pairs = 60 runs at T_{comf}=30) uses the deterministic fallback mapper to isolate the effect of natural-language preference on the downstream solver. Hurry-style personas ("I'm in a hurry, give me the shortest route") yield ρ=1.0 and recover B1. Neutral and heat-sensitive requests select progressively larger budgets ($\rho \approx 1.39$ and 1.50, respectively); in this low-contrast study area, both already reach the same heat-only route because the Pareto frontier saturates near a 4.5% realised detour. Thus the selected budgets remain context-dependent even when multiple budgets resolve to the same route. The same bounded interface accepts an LLM-derived sensitivity at deployment time, while Eq. (3) prevents pathological values.

Extended POI set for partner routes. For the partner-proposed subjective study and supplementary ρ analysis below, we extend the POI set with five additional sites snapped to the walk graph: Spartak Swimming Pool, the north-end fountain and Lake Vodna Pasha within South Park, Garibaldi Square, and Patriarch Evtimiy Square. These locations are not included in the 1,584-case full grid; they define waypoint-constrained routes that reflect how local residents actually traverse Sofia in summer.

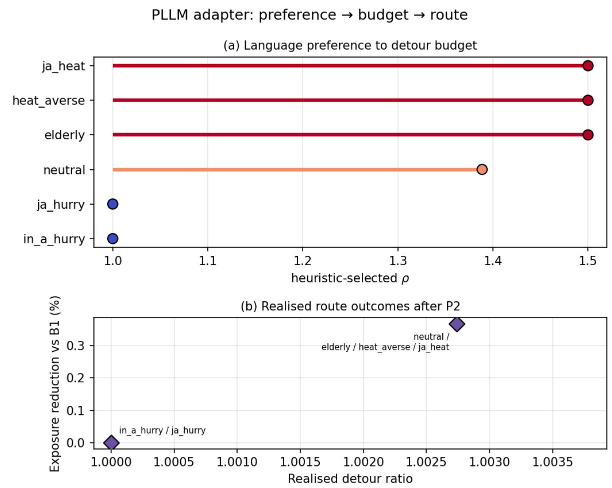

Figure 6. PLLM persona response. Panel (a) shows the deterministic fallback's selected detour budget for each natural-language persona. Panel (b) shows the resulting P2 outcomes: hurry personas recover B1, whereas neutral and heat-sensitive budgets reach the same heat-only endpoint because the local Pareto frontier saturates before their maximum budgets.

4.3 Partner-proposed routes and supplementary ρ analysis

To complement the full-grid evaluation, our partner institute specified five routes that local residents actually use in summer (Table 2). Each route is evaluated by chaining shortest or heat-aware paths through an ordered waypoint sequence (e.g., GW1 must pass Vitosha Boulevard). We run B1, P2 at $\rho \in \{1.0, 1.05, 1.10, 1.15, 1.20\}$, and PLLM (heuristic ρ from a fixed heat-averse message) on the same schedule as the main experiment (four hours × six July 2024 days), yielding 840 cases per T_{comf}. This finer ρ grid is intended as a zone-specific sensitivity check, not a replacement for the 1,584-case benchmark.

Only GW2 shows a non-zero exposure reduction within the tested ρ range (realised detour 1.2%, $r \approx 0.7\%$ at $\rho \geq 1.05$), consistent with the urban–park corridor offering more spatial heat contrast than the purely urban or park-internal pairs. GW3 confirms that uniform park microclimates limit detour-based gains even when the OD is confined to green space. These findings do not contradict the full-grid results; they localise where ρ-controlled routing can matter on routes that residents actually walk, and motivate the in-situ subjective study (section 4.4) as the check on whether algorithmic ρ choices align with lived navigation on those same corridors.

4.4 Subjective evaluation with Sofia-based walkers

The quantitative evaluation establishes that the proposed methods produce statistically significant heat reductions on the full 1,584-case grid; it does not show whether the resulting routes *feel* different to the people who actually walk them. Figure 7 shows the user interface of the proposed system. Given a natural-language request (e.g., "It's so hot today, please take me through shade and keep it cool"), the system generates a heat-exposure-aware walking route and contrasts it with the shortest route, which corresponds to what standard map services such as Google Maps provide. The interface also presents comparison metrics, route length, walking time, and cumulative heat

ID	From	To	Via / zone	$\ell(B1)$	$\max_\rho r$
GW1	Sveta Nedelya	NDK	Vitosha Blvd / urban	1,169 m	0%
GW2	NDK	Spartak Pool	South Park / urb.+park	3,270 m	0.7% ($\rho \geq 1.05$)
GW3	S.Park Fountain	Vodna Pasha	park interior	1,318 m	0%
GT1	Garibaldi Sq.	Pat. Evtimiy Sq.	Graf Ignatiev / tram	791 m	0%
GT2	Pat. Evtimiy Sq.	NDK	Pat. Evtimiy Blvd / trolley	1,013 m	0%

Table 2. Partner-proposed routes (GW = walking, GT = transit) and illustrative results at 15:00 LST on 2024-07-15 with $T_{\rm comf}$=30°C. Exposure reduction r is relative to the waypoint-constrained B1 baseline.

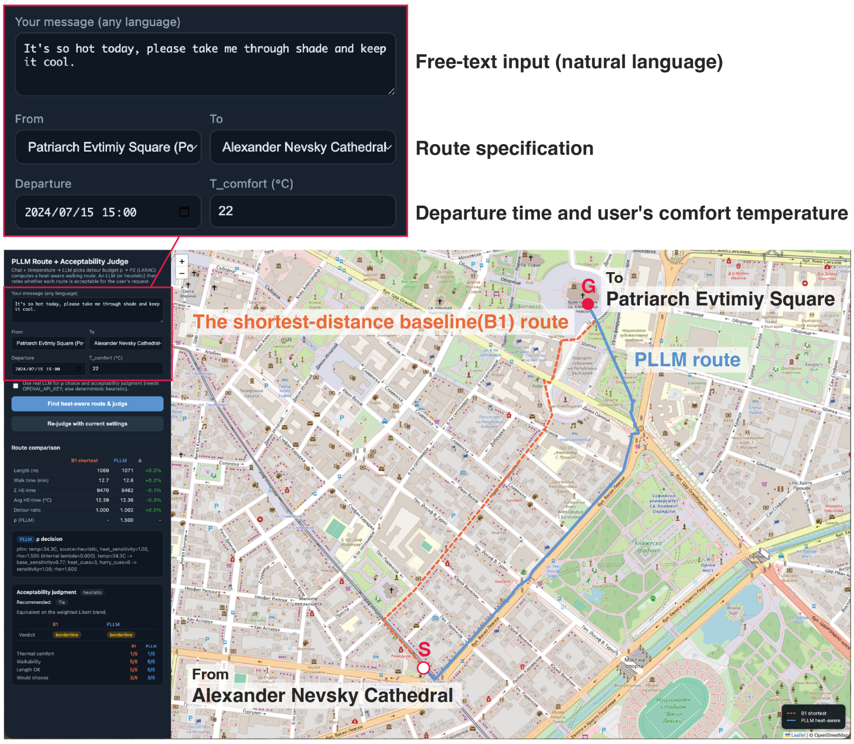

Figure 7. GUI of the proposed heat-exposure-aware routing system for the Patriarch Evtimiy Square–Alexander Nevsky Cathedral pair in Sofia. The solid blue line is the heat-avoiding route generated by the system; the dashed orange line is the conventional shortest route.

exposure, together with an LLM-based acceptability judgment for each route.

The protocol follows routes proposed by authors and covers five OD pairs with mandatory waypoints (Figure 8):

- Three **walking pairs**: GW1, Sveta Nedelya Church → NDK *via* Vitosha Boulevard (urban, ∼1.2 km); GW2, NDK → Spartak Swimming Pool *via* South Park (urban + park, ∼3.3 km); GW3, South Park Fountain → Lake Vodna Pasha within the park (park-only, ∼1.3 km).
- Two **transit pairs**: GT1, Garibaldy Square → Patriarch Evtimiy Square *via* Graf Ignatiev (tram, ∼0.8 km); GT2, Patriarch Evtimiy Square → NDK *via* Patriarch Evtimiy Boulevard (trolley, ∼1.0 km), where a walking-only route is compared against a walking + tram/trolley overlay; in-vehicle heat exposure is conservatively discounted (a near-zero contribution).

We set up a small in-situ study with n=3 Sofia-based residents (anonymised as R1–R3). The study was conducted on 10 July 2026 at around 10:00 local time (EEST) in Sofia. Among the OD pairs described above, three routes were selected for this study: Route 1: Patriarch Evtimiy Square → Alexander Nevsky Cathedral, Route 2: Alexander Nevsky Cathedral → South Park, and Route 3: Alexander Nevsky Cathedral → Lake Vodna Pasha. For each route, the participants were shown the shortest route (B1, dashed orange) and the route generated by the proposed system (PLLM, solid blue), and were asked for their impressions of both. The following comments were obtained:

1. *"Both paths are walkable. The orange offers a mixture of town square walkable zones and smaller streets. The blue one suggests walking on the boulevard sidewalk, which may include places exposed to more sunlight and heat. Both paths are walkable, but the orange one may be more pleasant and enjoyable."*
2. *"Both paths are walkable. The orange one offers a mixture of smaller cobblestone pavement alleys and main road sidewalks, meaning part of the journey would be in shade cover. The blue road goes through the old city center. The blue one also goes through 'Lozenets', and the parallel streets offer little difference in the walking experience; both are shade covered, comfortable and safe for pedestrians."*

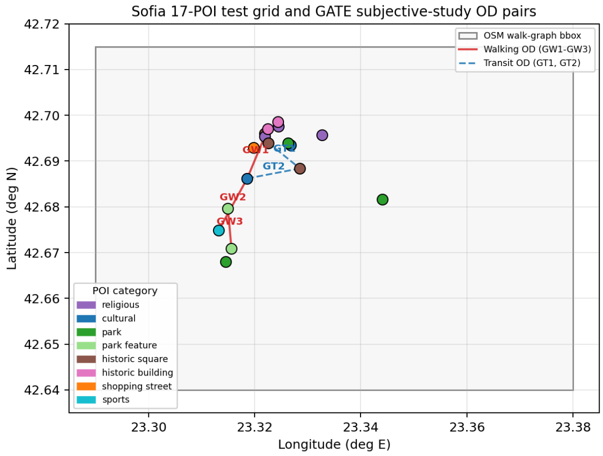

Figure 8. The 17-POI test grid in central Sofia (12 original sites plus five partner-proposed locations), the OSM walk-graph bounding box used for graph construction (section 3.2), and the five OD pairs of the subjective study (section 4.4) : three partner-proposed walking pairs (GW1–GW3, solid red) and two transit pairs (GT1–GT2, dashed blue). POI locations are colour-coded by category (legend); individual site names are omitted for legibility. The full-grid quantitative evaluation (section 4.2) uses all $\binom{12}{2} = 66$ pairs among the original 12 POIs only.

3. *"Both paths are walkable. The orange one suggests a detour into the neighborhood which avoids a larger street and walking near the bridge but also misses out on going through green spaces. Both paths offer shaded sidewalks and can be enjoyable. In this case the blue path might be better for seeing the cityscape."*

The participants' comments reveal both strengths and limitations of the heat-aware (PLLM, solid blue) routes. On the positive side, in Route 2 the blue route was described as passing through streets that are *shade covered, comfortable and safe for pedestrians"*, indicating that the system's heat-avoiding behaviour can align with pedestrians' perceived thermal comfort. In Route 3, the blue route was noted as passing through green spaces and as *better for seeing the cityscape"*, suggesting that heat-aware detours may also carry co-benefits for the touristic quality of the walk—an encouraging observation for a well-being-oriented tourism platform. All three participants further confirmed that the blue routes were walkable, i.e., the optimisation never produced impractical paths.

On the negative side, in Route 1 the blue route was perceived as following a boulevard sidewalk *exposed to more sunlight and heat"*, with the participant judging the shortest (orange) route as *more pleasant and enjoyable"*. This is a notable discrepancy: a route that is optimal with respect to the modelled cumulative heat exposure was subjectively perceived as the hotter option. Several factors may explain this gap. First, the microclimate field is defined on a regular grid and may not resolve street-level shading effects such as building shadows on narrow streets versus open boulevards; second, the study was conducted at around 10:00 local time, whereas the routing model assumed afternoon conditions, so the actual sun geometry differed from the modelled one; third, perceived comfort integrates factors beyond heat, street atmosphere, pavement type, and enjoyment, that the current objective function does not capture. In Route 2, the participants also observed that the parallel streets *"offer little difference in the walking experience"*, implying that in densely shaded areas the practical benefit of heat-aware rerouting may be marginal. Overall, these observations support the system's feasibility. Its routes are consistently walkable and, in some zones, perceived as comfortable and scenic, while highlighting that grid-based heat modelling can diverge from street-level perceived exposure.

5. Discussion

The Sofia central area exhibits a small spatial heat contrast: the heat-only path is only $\approx 4.5\%$ longer than B1, which limits the absolute heat reduction that any detour-based method can realise. The methodology nevertheless yields statistically significant improvements (Cohen's $d \in [-0.18, -0.35]$, all $p < 10^{-17}$ Holm-corrected) and – more importantly – it diagnoses heat-blind regressions by external services (B-ext, -11%). Cities with stronger spatial contrast (e.g., subtropical Hong Kong, where (Ma et al., 2025) reports up to 96% PET reduction with a 110% detour budget) should benefit substantially more from the same pipeline; the saturation we observe in Figure 5 is a property of the case study, not of the algorithm. In addition, the subjective evaluation suggested that grid-based heat modelling can diverge from street-level perceived exposure.

The PLLM design intentionally constrains the LLM's output to a single bounded scalar that is verified by a deterministic solver. This keeps the language interface expressive (free-text input) while keeping the safety profile of a classical optimiser (bounded output, reproducible behaviour, no hallucinated paths). The same pattern can be extended to additional dimensions – crowd avoidance, slope tolerance, accessibility constraints – by enriching the LLM's structured output with further bounded scalars and adding the corresponding edge-cost terms.

Limitations and future work. Limitations include (i) the synthetic microclimate field, which we plan to replace with sensor-derived WBGT once the partner institute's deployment delivers it; (ii) the small panel size (n=3) for the subjective study, intended only as a sanity check rather than a powered comparison; and (iii) the heat-blind treatment of in-vehicle public-transit segments. We plan to incorporate (a) sensor and crowd-flow data for dynamic re-routing, (b) higher-resolution shading information (e.g., building-shadow or sky-view-factor layers) and a broader walkability-aware objective that blends thermal comfort with other pedestrian preferences, (c) time-dependent diurnal forecasts for predictive routing earlier in the day, (d) accessibility constraints (slope, surface) for vulnerable users, and (e) a federated training stage for the LLM adapter so that the system can adapt to city-specific phrasing and culture without centralising personal data.

6. Conclusion

We proposed a Well-Being-Centric Walkable Tourism Platform that combines an OSM pedestrian graph, a Sofia microclimate field, and a walkability layer with an AI agent that translates free-text requests into a ρ-detour-constrained heat-aware route. On 1,584 OD cases the heat-aware engine yields statistically significant exposure reductions (up to 0.81% on a hard-contrast central area, all $p < 10^{-17}$) and – crucially – exposes heat-blind regressions of an off-the-shelf external service (Google Directions, -11% in cumulative heat exposure). The LLM-driven preference module reliably steers the same solver into a B1-recovering "hurry" regime (ρ=1.0) or a heat-only "heat-averse" regime (ρ=1.5), giving users a natural-language handle on the detour-vs-comfort trade-off without exposing the underlying Lagrangian. A supplementary analysis on five partner-proposed routes (840 cases, finer ρ grid) localises zone-dependent sensitivity, and a small in-situ study with three Sofia-based walkers across three walking and two transit pairs is set up to validate that the routing rationale aligns with local lived experience. The framework is data-source-agnostic and we expect substantially larger absolute gains in cities with stronger spatial heat contrast.

Acknowledgements

The Sofia microclimate field, walkability layer, and on-site logistics for the participant-walked subjective evaluation are kindly provided in collaboration with our partner research institute. The authors thank the three local walkers (anonymised as R1–R3) for their participation.

References

Boeing, G., 2017. OSMnx: New methods for acquiring, constructing, analyzing, and visualizing complex street networks. *Computers, Environment and Urban Systems*, 65, 126–139.

Dijkstra, E. W., 1959. A note on two problems in connexion with graphs. *Numerische Mathematik*, 1(1), 269–271.

Gretzel, U., Sigala, M., Xiang, Z., Koo, C., 2020. Smart tourism: foundations and developments. *Electronic Markets*, 30(1), 7–18. doi.org/10.1007/s12525-015-0196-8.

Hagberg, A. A., Schult, D. A., Swart, P. J., 2008. Exploring network structure, dynamics, and function using NetworkX. *Proc. 7th Python in Science Conf. (SciPy 2008)*, 11–15.

Holm, S., 1979. A simple sequentially rejective multiple test procedure. *Scandinavian Journal of Statistics*, 6(2), 65–70.

Honey, M., Frenkiel, K., 2021. *Overtourism: Lessons for a Better Future*. Princeton University Press.

Huber, J., Ludwig, C., Foshag, K., Kolaxidis, N., Zipf, A., Lautenbach, S., 2025. Accessibility for pedestrians under heat stress – the example of Heidelberg, Germany. *AGILE GIScience Ser.*, 6, 4. doi.org/10.5194/agile-giss-6-4-2025.

Isoda, S., Hidaka, M., Matsuda, Y., Suwa, H., Yasumoto, K., 2020. Timeliness-aware on-site planning method for tour navigation. *Smart Cities*, 3(4), 1383–1404. doi.org/10.3390/smartcities3040066.

Jüttner, A., Szviatovszki, B., Mécs, I., Rajkó, Z., 2001. Lagrange relaxation based method for the QoS routing problem. *Proc. IEEE INFOCOM*, 859–868.

Kawanaka, S., Matsuda, Y., Suwa, H., Fujimoto, M., Arakawa, Y., Yasumoto, K., 2020. Gamified participatory sensing in tourism: An experimental study of the effects on tourist behavior and satisfaction. *Smart Cities*, 3(3), 736–757. doi.org/10.3390/smartcities3030037.

Kuroki, S., Nakagawa, M., Yoshida, S., Koyama, Y., Kozuno, T., 2026. LAPPI: Interactive Optimization With LLM-Assisted Preference-Based Problem Instantiation. *IEEE Access*, 14, 49207-49224.

Lemke, B., Kjellstrom, T., 2012. Calculating workplace WBGT from meteorological data: a tool for climate change assessment. *Industrial Health*, 50(4), 267–278.

Lewis, P., Perez, E., Piktus, A., Petroni, F., Karpukhin, V., Goyal, N., Küttler, H., Lewis, M., Yih, W., Rocktäschel, T., Riedel, S., Kiela, D., 2020. Retrieval-augmented generation for knowledge-intensive NLP tasks. *Adv. Neural Inf. Process. Syst. (NeurIPS)*.

Lim, K. H., Chan, J., Leckie, C., Karunasekera, S., 2015. Personalized tour recommendation based on user interests and points of interest visit durations. *Proceedings of the 24th International Conference on Artificial Intelligence*, IJCAI'15, AAAI Press, 1778–1784.

Ma, X., Zeng, T., de Dear, R., Xie, Y., Yuan, C., Lu, S., 2025. Active route choice to minimize pedestrian thermal discomfort in a high-density subtropical city. *Sustainable Cities and Society*, 131, 106697. doi.org/10.1016/j.scs.2025.106697.

Matsuda, Y., Kawanaka, S., Suwa, H., Arakawa, Y., Yasumoto, K., 2022. ParMoSense: Scenario-based participatory mobile urban sensing platform with user motivation engine. *Sensors and Materials*, 34(8), 3063–3091. doi.org/10.18494/SAM3961.

Melnikov, V. R., Christopoulos, G. I., Krzhizhanovskaya, V. V., Lees, M. H., Sloot, P. M. A., 2022. Behavioural thermal regulation explains pedestrian path choices in hot urban environments. *Scientific Reports*, 12, 2701. doi.org/10.1038/s41598-022-06383-5.

OpenStreetMap contributors, 2024. Planet OSM. openstreetmap.org.

Peeters, P., Gössling, S., Klijs, J., Milano, C., Novelli, M., Dijkmans, C., Postma, A., 2018. Research for TRAN committee – overtourism: impact and possible policy responses. Technical report, European Parliament, Policy Department for Structural and Cohesion Policies.

Thom, E. C., 1959. The discomfort index. *Weatherwise*, 12(2), 57–61.

UNWTO, 2018. "Overtourism"? Understanding and Managing Urban Tourism Growth beyond Perceptions: Executive Summary. World Tourism Organization, Madrid.

Yaglou, C. P., Minard, D., 1957. Control of heat casualties at military training centers. *Archives of Industrial Health*, 16(4), 302–316.

Yahi, A., Chassang, A., Raynaud, L., Duthil, H., Chau, D. H. P., 2015. Aurigo: an interactive tour planner for personalized itineraries. *Proceedings of the 20th International Conference on Intelligent User Interfaces*, IUI '15, Association for Computing Machinery, New York, NY, USA, 275–285.